Can. J. Chem. Downloaded from cdnsciencepub.com by YORK UNIV on 07/12/24
For personal use only. This Just-IN manuscript is the accepted manuscript prior to copy editing and page composition. It may differ from the final official version of record.

Tuning Phenolic Hemicyanines for Ratiometric DNA Sensing and Live Cell Nuclear Bioimaging Applications

Abigail J. Van Riesen,[†] Keenan T. Regan,[†] Baylie Kalnitsky,[†] Aron A. Shoara,[‡] Sladjana Slavkovic,[‡] Zachary R. Churcher,[‡] Philip E. Johnson,[‡,*] Giammarco Nebbioso,[‡] Sergey N. Krylov,[‡,*] and Richard A. Manderville[†,*]

[†]Departments of Chemistry and Toxicology, University of Guelph, 50 Stone Road East, Guelph, Ontario, Canada N1G 2W1

[‡]Department of Chemistry, York University, 4700 Keele Street, Toronto, Ontario, Canada M3J 1P3

Corresponding Authors

[‡]P.E.J. e-mail: pjohnson@yorku.ca

[‡]S.N.K. e-mail: skrylov@yorku.ca

[†]R.A.M. e-mail: rmanderv@uoguelph.ca

© The Author(s) or their Institution(s)

Can. J. Chem. Downloaded from cdnsciencepub.com by YORK UNIV on 07/12/24
For personal use only. This Just-IN manuscript is the accepted manuscript prior to copy editing and page composition. It may differ from the final official version of record.

Abstract: Activatable fluorescent probes with turn-on emission in response to a biological target can reduce the background signal and improve the detection limit needed for biosensor and bioimaging resolution. Turn-on probes with dual emission (ratiometric probes) have further advantages, as they have self-calibration ability for more reliable detection. Herein we demonstrate the tunability of the phenolic hemicyanine (HC) scaffold for both DNA biosensing and bioimaging applications using the quinine-binding DNA aptamer (MN4) as a host-guest biosensor platform and live ovarian cancer cells for nuclear imaging. The DNA aptamer MN4 contains a three-way junction (3WJ) consisting of a hydrophobic branch point connecting three double-stranded stems. Phenolic HCs bearing electron-withdrawing halogen substituents (FPhOBtz and Cl_2PhOBTz) bind to the 3WJ of MN4 as the phenolate with strong turn-on emission. Subsequent displacement of the phenolate by the quinine target causes a turn-off emission response. In contrast, the parent phenolic HC (PhOBtz) and those bearing electron-donating groups (Me_2PhOBtz and $(MeO)_2$PhOBtz) exhibit dual (phenol and phenolate) fluorescence upon MN4 binding. Phenol excitation generates phenolate emission by an excited-state proton transfer (ESPT) process with DNA components serving as the proton acceptor. Quinine displacement of PhOBtz from the 3WJ of MN4 affords a turn-on ratiometric response with preferential light-up of phenol emission. The ability of the phenolic HCs to serve as cellular nuclear stains further highlights the tunability of the phenolic HC probes with the Cl_2PhOBtz analog displaying superior staining ability. The simplicity and tunability of phenolic HCs make them attractive fluorescent probes for DNA sensing and bioimaging applications.

© The Author(s) or their Institution(s)

Key words: Fluorescent probe, ratiometric detection, DNA biosensing, live cell nuclear imaging, excited-state proton transfer (ESPT), DNA aptamer, phenolic hemicyanine dyes

Can. J. Chem. Downloaded from cdnsciencepub.com by YORK UNIV on 07/12/24
For personal use only. This Just-IN manuscript is the accepted manuscript prior to copy editing and page composition. It may differ from the final official version of record.

© The Author(s) or their Institution(s)

Can. J. Chem. Downloaded from cdnsciencepub.com by YORK UNIV on 07/12/24
For personal use only. This Just-IN manuscript is the accepted manuscript prior to copy editing and page composition. It may differ from the final official version of record.

Introduction

Fluorescent probes with molecular rotor properties are widely used for DNA sensing applications. The dyes display quenched fluorescence in water, which intensifies upon biopolymer binding in a more rigid and hydrophobic microenvironment.[1,2] Hemicyanine (HC) dyes, featuring aromatic donors attached to a cationic acceptor via a vinyl linkage, provide molecular rotor character and a tunable platform for fluorescent detection strategies.[3,4] Typically, nitrogen analogs (*N*-donors) like dialkylaniline derivatives are attached to cationic *N*-alkylbenzothiazolium (Btz) or indolenium (Ind) acceptors.[5-7] However, most *N*-donor HCs offer a single fluorescent peak for intensity-based sensing, which introduces drawbacks like instrument dependence and probe concentration issues.[8,9]

To overcome these limitations, dual-emission fluorescent probes have gained attention for providing ratiometric sensing, with self-calibration ability independent of instrument settings and probe concentrations.[8,9] This approach is fundamentally different from a Förster resonance energy transfer (FRET)-based strategy, which requires the presence of two dyes (donor and acceptor) to be within a specific distance range.[10,11] Single probes for ratiometric sensing include twisted intramolecular charge transfer (TICT)[12,13] and excited-state intramolecular proton transfer (ESIPT) systems.[14,15] TICT probes produce a locally excited planar form (LE), which can undergo TICT to produce the twisted structure with a larger dipole moment and red-shifted emission. In this system the LE state is emissive, whereas the TICT state may not be, which can hinder ratiometric analysis.[9] Classic ESIPT-active fluorophores, such as the 2-(2′-hydroxyphenyl) benzazole (HBX) series,[16] undergo photoinduced tautomerization from a ground-state enol form to an excited-state keto form to afford a large Stokes-shifted fluorescence. However, attachment of HBX derivatives to cationic Btz or Ind acceptors to produce ESIPT-active HCs strongly favours keto emission precluding observation of enol emission for ratiometric sensing.[17]

© The Author(s) or their Institution(s)

Can. J. Chem. Downloaded from cdnsciencepub.com by YORK UNIV on 07/12/24
For personal use only. This Just-IN manuscript is the accepted manuscript prior to copy editing and page composition. It may differ from the final official version of record.

Herein, we introduce excited-state proton transfer (ESPT) as a strategy for ratiometric host-guest DNA sensing, utilizing HCs with *O*-donor phenolic groups.[18-20] These phenolic HCs, ideal for pH sensing due to absorbance wavelength changes between the phenol and phenolate forms, are employed for host-guest DNA biosensing, focusing on alkaloid detection using the quinine-binding aptamer MN4 (Figure 1).[19-21] Our previous studies highlighted light-up fluorescence of phenolic HCs bearing electron-withdrawing halogen substituents to favor single phenolate absorbance/emission upon MN4 binding. Consequently, these probes provided a turn-off emission readout upon dye displacement by quinine or cocaine.[19,20] We now draw comparison between *O*-donor HCs which favor phenolate emission with the parent phenolic HC (PhOBtz) and those bearing electron-donating substituents ($(MeO)_2$PhOBtz and Me_2PhOBTz, Figure 1). The latter dyes exhibit both phenol and phenolate emission upon MN4 binding and permit comparison of nuclear DNA staining by the phenolate versus the phenolic forms in live cells. Our results introduce ESPT as a ratiometric mechanism for host-guest DNA biosensing, which is distinct from ESIPT because the *O*-donor HCs lack an attached proton acceptor. Instead, basic DNA components (phosphate or nucleobases) within the 3WJ of MN4 accept the proton from the excited phenolic HC through an intermolecular ESPT process to afford dual-band (phenolic and phenolate) emission. Our results for ESPT within a DNA microenvironment permit comparison to ESPT within green fluorescent protein (GFP) and showcase phenolic HCs as attractive fluorescent probes for DNA biosensing and bioimaging applications.

© The Author(s) or their Institution(s)

Can. J. Chem. Downloaded from cdnsciencepub.com by YORK UNIV on 07/12/24
For personal use only. This Just-IN manuscript is the accepted manuscript prior to copy editing and page composition. It may differ from the final official version of record.

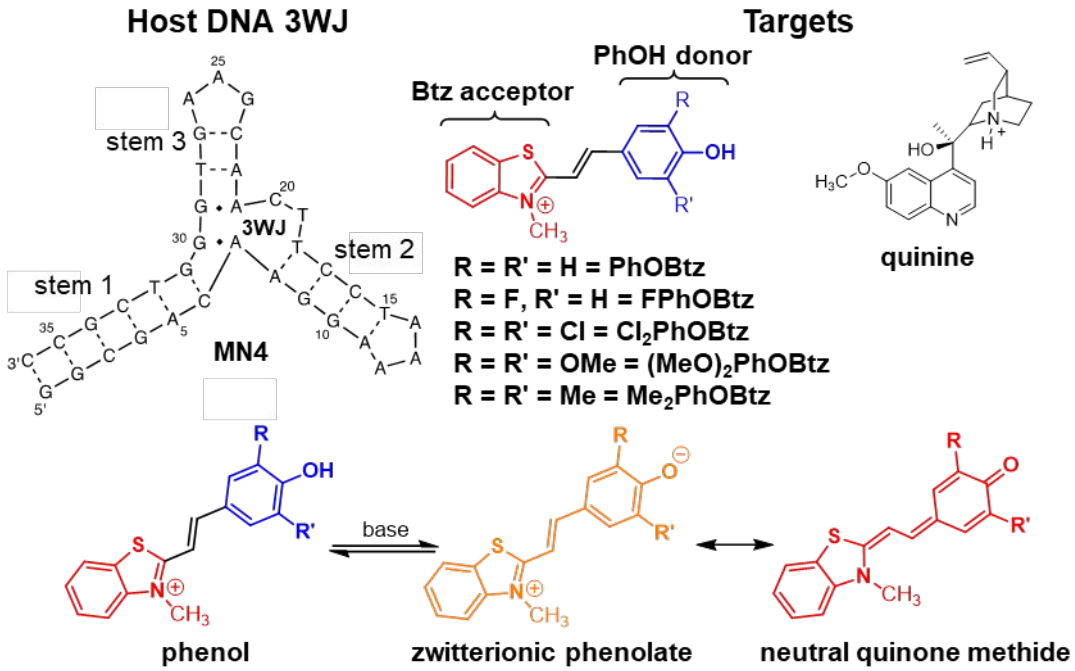


Figure 1. Structures of host 3WJ MN4 DNA aptamer, phenolic hemicyanine dyes and quinine targets.

Materials and Methods

General. 2-Methylbenzothiazole, methyl iodide, 4-hydroxy-benzaldehydes, quinine hemisulfate monohydrate, and the sample of MN4 were obtained from commercial sources and used as received. Treatment of 2-methylbenzothiazole with methyl iodide (1.5 equiv.) in acetonitrile at reflux was used to prepare *N*-methyl-2-methylbenzothiazolium iodide, as described previously.[18,19] NMR experiments were conducted on a 600 MHz Bruker Avance spectrometer equipped with an HCP triple resonance probe. Mass spectra were acquired on an Agilent Q-TOF high-resolution (HRMS) instrument, using an electrospray ionization source.

Hemicyanine dye synthesis. HC dyes were synthesized by the Knoevenagel condensation reaction between the various 4-hydroxy-benzaldehydes (1.60 mmol, 1.0 equiv) with *N*-methyl-2-methyl-benzothiazolium iodide (1.75 mmol, 1.1 equiv), catalyzed by piperidine (0.16 mmol, 0.1 equiv) in

© The Author(s) or their Institution(s)

Can. J. Chem. Downloaded from cdnsciencepub.com by YORK UNIV on 07/12/24
For personal use only. This Just-IN manuscript is the accepted manuscript prior to copy editing and page composition. It may differ from the final official version of record.

ethanol (0.2 M) at 80 ˚C using an oil bath, as outlined previously for the synthesis of PhOBtz,[18] Cl_2PhOBtz[18] and FPhOBtz.[19] Following precipitation with diethyl ether, the compounds were isolated as coloured powders. Copies of NMR and HRMS spectra for Me_2PhOBtz and $(MeO)_2$PhOBtz are available in Supplemental Material (SM).

UV-vis Measurements. All UV-vis spectra were obtained on Cary 100- and 300-Bio UV-vis spectrophotometer. Stock solutions of HCs (2 mM) were prepared in dimethyl sulfoxide (DMSO). UV-vis titrations with 5 μM HC in PBS buffer (pH 7.4) for MN4 binding were carried out at 20 ˚C with additions (0.25 equiv.) of MN4 up to 20 μM (4 equiv.) with manual mixing of the samples. Displacement experiments were carried out by pre-binding the HC to MN4 to create the dye-DNA complex in PBS buffer. Subsequent HC displacement in response to addition of 10-30 equivalents quinine were carried out. The UV-vis spectra were recorded 2 minutes after manual mixing of the samples. The phenolic pK_a values for HCs were determined spectrophotometrically at 21 ˚C in 0.05 M aqueous buffer containing 0.2 M KCl, as previously outlined for PhOBtz,[18] FPhOBtz[19] and FPhOInd.[22]

Fluorescence Measurements. All fluorescence spectra were acquired on a Cary Eclipse Fluorescence spectrophotometer in quartz cells (108.002F-QS) with a path length of 10 × 2 mm at 20 ˚C. Stock solutions of HCs (2 mM) were prepared in DMSO. Fluorescence titrations with 1 μM HC in PBS buffer (pH 7.4) at 20 ˚C were carried out with systematic addition up to 2 μM (2 equiv) of MN4. The fluorescence spectra were recorded 2 minutes after manual mixing of the samples. Relative fluorescence quantum yield (Φ_{fl}) of MN4-bound phenolate for each HC in PBS buffer at 20 ˚C were measured using quinine sulfate in 0.1 N sulfuric acid as the fluorescence standard solution.[19] HC samples were mixed with 3-fold MN4 concentrations and the molar ratio of HC:MN4 were kept constant throughout the experiment. The photomultiplier tube voltage, signal-to-noise ratio, and spectral bandwidth parameters were also kept constant in all experiments. All MN4 samples were heated in a 95 ˚C water bath for 3

© The Author(s) or their Institution(s)

Can. J. Chem. Downloaded from cdnsciencepub.com by YORK UNIV on 07/12/24
For personal use only. This Just-IN manuscript is the accepted manuscript prior to copy editing and page composition. It may differ from the final official version of record.

min and cooled in an ice-water bath for 5 min to allow the aptamer to anneal prior to each experiment. The integrated emission intensities were plotted against the integrated excitation (absorption) intensities. The obtained linear slope was used to quantify the relative quantum yield values using OriginPro 2016 software package. Emission titrations monitoring displacement of PhOBtz (5 μM) from MN4 (10 μM) at pH 6.5 in 20 mM MES buffer mediated by quinine addition (up to 6 equiv.) were carried out at 21 ˚C. Emission spectra ($\lambda_{excitation}$ = 400 nm) were recorded 2 min after manual mixing of the samples. Limits of detection (LOD) were determined via $3.3\,\sigma/m$ where σ is the standard error of the y-intercept of the regression curve and m is the slope of the linear range.

Isothermal Titration Calorimetry. ITC binding experiments were performed using a MicroCal VP-ITC instrument in a manner similar to what has been previously described.[19,22,23] The MN4 sample was dissolved in ~1 mL ddH_2O per 1 micromole scale synthesis, then exchanged 3 times against 1 M NaCl and then 4-6 times against ddH_2O. The MN4 samples were finally exchanged 3-4 times against the buffer (20 mM TRIS, pH 7.4), 140 mM NaCl, 5 mM KCl). The MN4 concentration was measured using UV spectroscopy and the known extinction coefficient provided by the manufacturer. Samples were degassed before analysis with a MicroCal Thermo Vac unit for 5 minutes. All experiments were corrected for the heat of dilution of the titrant. To perform experiments in as low a concentration of DMSO as possible, titrations were performed 'in reverse" with the ligand samples in the cell and the DNA aptamer as the titrant, in the needle. All aptamer samples were heated in a 95 ˚C water bath for 3-5 minutes and cooled in an ice water bath for at least 10 minutes prior to use in a binding experiment to allow the DNA aptamer to anneal in an intramolecular fashion. The binding experiments were performed at 15 ˚C with the aptamer solution at 0.312 mM using a ligand concentration in the cell of 20 μM. The HC was diluted to the experimental concentration with the buffer to a final DMSO

© The Author(s) or their Institution(s)

Can. J. Chem. Downloaded from cdnsciencepub.com by YORK UNIV on 07/12/24
For personal use only. This Just-IN manuscript is the accepted manuscript prior to copy editing and page composition. It may differ from the final official version of record.

concentration of 1% (v/v). DMSO was added to the aptamer solution and the reference cell at the same concentration to avoid buffer mismatch. ITC data were fit to a one-site binding model using the manufacturer provided Origin 7 software.

NMR Experiments. The MN4 sample was heated in boiling water for 1 min, and then cooled in an ice-water bath for at least 5 min to favour intramolecular folding of the aptamer prior to performing NMR experiments. 1D ^{1}H spectra were acquired in 140 mM NaCl, 10 mM $Na_xH_yPO_4$ at pH 6.8 in 10% $^{2}H_2O$/90% $^{1}H_2O$ at 5 ˚C in a manner described previously.[19,20,24] The concentration of the MN4 aptamer in the buffer was 1.4 mM, at a volume of 600 μL. For NMR experiments, the Me_2PhOBtz dye was dissolved in DMSO-d_6 (99.96%). Me_2PhOBtz was titrated into the MN4 sample to a 1:1 ratio of aptamer:ligand, bringing the final DMSO content of the sample to ~5%.

Cellular Imaging Experiments. Ovarian cancer cells SKOV3 were donated by Dr. Peng's laboratory (York University) who sourced them from the American Tissue Culture Collection (catalog number HTB-77). Cells were supplemented with 10% fetal bovine serum (Gibco, Grand Island, NY, USA, Cat. No: 12483–020). Cells were cultured in 60-mm (Sarstedt AG&Co, Numbrecht, Germany, Cat. No: 83.3901) and 35-mm dishes for imaging (Nest Biotechnology Co, Wuxi, Jiangsu, China, Cat. No: 706001) at 37 ˚C in a humidified incubator with 5% CO_2. Cells were cultured until they reached approximately 70% confluence and then incubated with 1.2 mL of 3 μM HC $(MeO)_2$PhOBtz, FPhOBtz, and Cl_2PhOBtz) for 30 minutes at 37 ˚C. Imaging was performed with an epifluorescence Leica DMi8 high-throughput cell-imaging system (7.81 ms exposure time). Cells were observed with both brightfield (BF) (apochromatic HC PL APO 10x/0.45 objective lens) and fluorescence (FITC filter cube was used for $(MeO)_2$PhOBtz , while a RHOD filter cube was used for FPhOBtz, and Cl_2PhOBtz) microscopy. In total, a set of one BF and one fluorescence images were obtained for each dye. Using

© The Author(s) or their Institution(s)

Can. J. Chem. Downloaded from cdnsciencepub.com by YORK UNIV on 07/12/24
For personal use only. This Just-IN manuscript is the accepted manuscript prior to copy editing and page composition. It may differ from the final official version of record.

the open-source program Fiji, a composite image was obtained for each dye by overlapping the BF and fluorescence images.

Table 1. Physicochemical Properties of Phenolic Hemicyanine Dyes.

Dye	pK_a	ΔpK_a[a]	pK_a*[b]	λ_{max}^{PhOH}, ε_{max}[c]	λ_{max}^{PhO-}, ε_{max}[c]
PhOBtz	7.76 ± 0.03	2.22	0.25	404, 70,248	493, 87,125
FPhOBtz[d]	6.60 ± 0.05	2.10	–0.67	398, 64,183	485, 88,095
Cl_2PhOBtz	4.28 ± 0.07	2.53	ND	391, 46,910	481, 68,900
$(MeO)_2$PhOBtz	7.52 ± 0.05	2.46	1.44	425, 42,792	552, 92,810
Me_2PhOBtz	7.91 ± 0.04	2.69	0.38	412, 69,497	528, 93,650

[a]ΔpK_a = pK_a (parent phenol) – pK_a (HC dye), i.e. ΔpK_a for PhOBtz = 9.98-7.76 = 2.22. [b]Excited-state pK_a* values were determined using the Förster cycle where pK_a* = pK_a – $N_A h$c/2.303RT [$\tilde{\nu}_{ArOH} - \tilde{\nu}_{ArO-}$] in which the overlay of the fluorescence and absorbance spectra of the acidic and basic solutions are used to determine $\Delta\tilde{\nu}$. [c]λ_{max} values in nanometers (nm), ε_{max} values in $cm^{-1}M^{-1}$. [d]pK_a and optical data for FPhOBtz taken from ref. 19.

Results and Discussion

Dye Physicochemical Properties. In aqueous buffer, FPhOBtz possesses a phenolic pK_a ≈ 6.6 with phenol and phenolate absorbances at ~ 398 and 485 nm, respectively (Table 1). UV-vis pH-titrations for the other *O*-donor HCs are given in Figure S1 (SM). Dye pK_a values were compared to literature pK_a values of the parent phenol to afford ΔpK_a values in the 2.1-2.7 range (Table 1). The vinyl-Btz moiety is electron-withdrawing and stabilizes the phenolate to lower the pK_a compared to the parent phenol. For para-substituted phenols the Hammett substituent constant σ^- provides a means to gauge the magnitude of the electron-withdrawing ability of the vinyl-Btz. As presented previously for σ^- determination for phenols containing para-purine substituents,[25] the equation pK_a = pK_a of parent phenol

© The Author(s) or their Institution(s)

Can. J. Chem. Downloaded from cdnsciencepub.com by YORK UNIV on 07/12/24
For personal use only. This Just-IN manuscript is the accepted manuscript prior to copy editing and page composition. It may differ from the final official version of record.

– 2.23(Σσ) derived by Biggs and Robinson[26] afforded a σ^- of 1.0 for vinyl-Btz. This value indicates that the electron-withdrawing capability of vinyl-Btz is similar to an aldehyde (σ^- = 1.03), stronger than an ester (σ^- = 0.75), but not as strong as NO_2 (σ^- = 1.27).[27]

The photoacidity of the HCs was initially examined in MeOH. Only Cl_2PhOBtz displayed obvious ESPT to afford phenolate emission from phenol excitation in pure MeOH. For the other *O*-donor HCs, excited-state pK_a* values were determined using the Förster cycle (Table 1).[28,29] Values ranged from a low of –0.67 for FPhOBtz to a high of +1.44 for $(MeO)_2$PhOBtz. A value for Cl_2PhOBtz, which is a strong photoacid capable of protonating MeOH, could not be determined due to ESPT mediated by the dye in aqueous media at low pH.

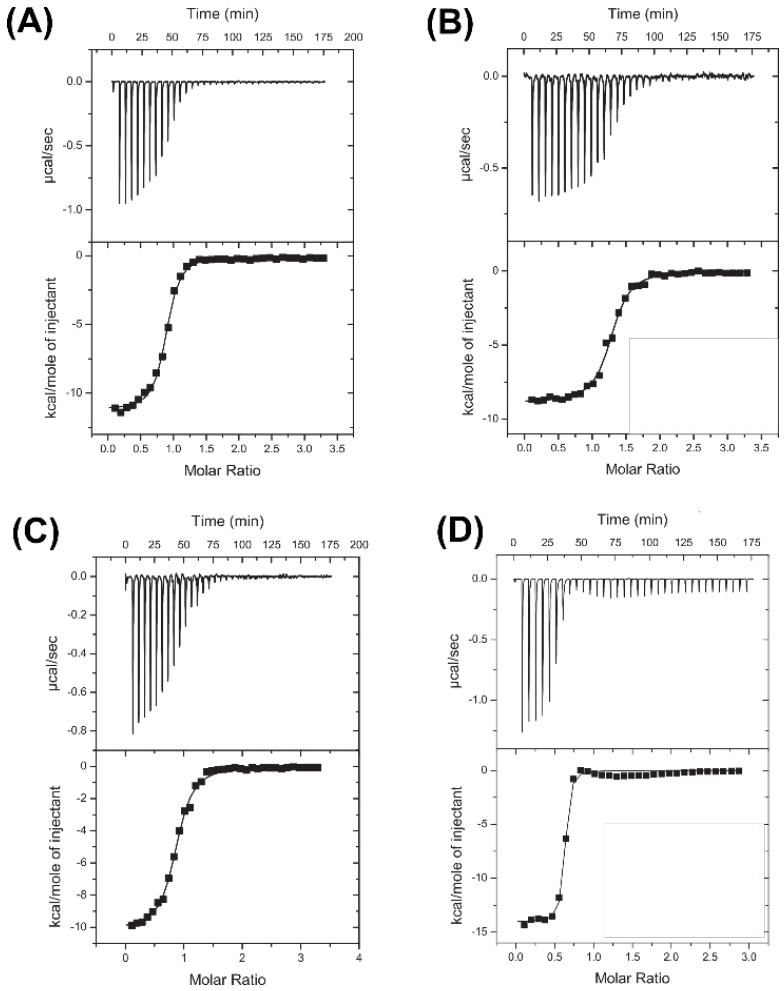
The negative solvatochromism for the HC dyes in protic solvents (H_2O, MeOH, EtOH and isopropanol (IPA)) was also examined by monitoring changes in λ_{max} versus solvent polarity.[19] For FPhOBtz, Cl_2PhOBtz and PhOBTz, gradual wavelength shifts to the red were observed in response to decreased solvent polarity (Figure S2A). For these dyes, the phenolate λ_{max} values provided linear correlations with the empirical solvent polarity scale $E_T(30)$ (Figure S2B).[30] However, for $(MeO)_2$PhOBtz and Me_2PhOBtz derivatives bearing electron-donating substituents, which stabilize the neutral quinone methide (QM) resonance structure (Figure 1), poor correlations between λ_{max} and $E_T(30)$ were obtained (Figure S2B), as it was not possible to distinguish the polarity of EtOH from IPA using their negative solvatochromic properties.

Hemicyanine binding to MN4. The affinity of the phenolic HCs toward MN4 were determined using ITC to establish thermodynamic parameters and dissociation constants (K_d) under conditions previously employed for FPhOBtz and quinine binding to the aptamer (Figure 2, Table 2).[19] The HCs FPhOBtz, PhOBtz, Cl_2PhOBtz and $(MeO)_2$PhOBtz all displayed similar binding affinity to MN4 with K_d values in the 0.25-0.52 μM range (Table 2). However, the Me_2PhOBtz analog (Figure 2D) displayed a 10.5-fold

© The Author(s) or their Institution(s)

Can. J. Chem. Downloaded from cdnsciencepub.com by YORK UNIV on 07/12/24
For personal use only. This Just-IN manuscript is the accepted manuscript prior to copy editing and page composition. It may differ from the final official version of record.

increase in binding affinity with a K_d of 0.04 μM. MN4 binding by the HCs was also examined using UV-vis, fluorescence and ^{1}H NMR. As presented previously, FPhOBtz binds to the 3WJ motif of MN4 at pH 7.4 as the phenolate with the absorbance of the free dye at 485 nm shifting to 540 nm ($\Delta\lambda_{max}$ = 55 nm) with phenolate fluorescence at ~ 580 nm increasing >600-fold with a fluorescence quantum yield (Φ_{fl}) = 0.76 for the MN4-bound dye. Similar results were obtained for MN4 binding by Cl_2PhOBtz (pK_a = 4.28, Table 1). In this case, the free phenolate absorbance at 481 nm shifted to 534 nm ($\Delta\lambda_{max}$ = 53 nm) with similar intensity (Figure S3A, SM). The phenolate fluorescence for Cl_2PhOBtz at 579 nm increased by ~ 400-fold for the MN4-bound dye (Figure S3B) and had Φ_{fl} = 0.50 for a brightness ($\varepsilon\Phi_{fl}$) = 34,450 cm^{-1}M^{-1}, which essentially matches the brightness of the commercial PicoGreen dye bound to calf thymus DNA (brightness ~ 35,000 cm^{-1}M^{-1}).[31]



© The Author(s) or their Institution(s)

Can. J. Chem. Downloaded from cdnsciencepub.com by YORK UNIV on 07/12/24
For personal use only. This Just-IN manuscript is the accepted manuscript prior to copy editing and page composition. It may differ from the final official version of record.

Figure 2. ITC thermograms showing MN4 binding by (A) PhOBtz, (B) $(MeO)_2$PhOBtz, (C) Cl_2PhOBtz, (D) Me_2PhOBtz. For each titration, the top trace is the raw titration data showing the heat resulting from each injection of ligand into aptamer solution. The bottom shows the integrated heat plot after correcting for the heat of dilution. Data was acquired in 20 mM Tris (pH 7.4), 140 mM NaCl, 5 mM KCl with 1% (v/v) DMSO at 15 ˚C.

Table 2. ITC Binding Affinity, Thermodynamic Parameters and Fluorescent Properties of Dye Binding to MN4.

Dye	K_d (μM)[a]	ΔH^b	$-T\Delta S^b$	$\lambda_{ex}/\lambda_{em}$[c]	$\lambda_{ex}/\lambda_{em}$[d]	Φ_{fl}[e]
PhOBtz	0.25 ± 0.01	–11.2 ± 1	2.8 ± 0.1	411/519	545/575	0.18
FPhOBtz[f]	0.42 ± 0.01	–9.3 ± 1	0.9 ± 0.5	–	540/580	0.76
Cl_2PhOBtz	0.52 ± 0.04	–10.2 ± 1	1.8 ± 0.1	–	532/579	0.50
$(MeO)_2$PhOBtz	0.31 ± 0.03	–8.9 ± 0.1	3.1 ± 0.2	466/552	552/620	0.01
Me_2PhOBtz	0.04 ± 0.01	–15.0 ± 1	4.2 ± 0.2	457/524	570/589	0.05

[a]ITC binding experiments were performed at 15 ˚C in 20 mM TRIS (pH 7.4), 140 mM KCl and K_d values are averages of 2-3 individual experiments. [b]Values in kcal/mol extracted from the ITC binding data. [c]Excitation and emission maxima (nm) for the neutral phenol bound to MN4. [d]Excitation and emission maxima (nm) for the phenolate bound to MN4. [e]Quantum yield for phenolate emission of the dye bound to MN4 at 20 ˚C. [f]Data for FPhOBtz taken from ref. 19.

The HC dyes PhOBtz, $(MeO)_2$PhOBtz and Me_2PhOBtz with pK_a values > 7.4 (Table 1) displayed both phenol and phenolate absorbances at pH 7.4 that changed in wavelength and intensity upon MN4 binding, as exemplified for Me_2PhOBtz (Figure 3A). In pH 7.4 PBS, free Me_2PhOBtz exhibits phenol absorbance at 417 nm and phenolate absorbance at 535 nm (solid orange trace). Addition of MN4

© The Author(s) or their Institution(s)

Can. J. Chem. Downloaded from cdnsciencepub.com by YORK UNIV on 07/12/24
For personal use only. This Just-IN manuscript is the accepted manuscript prior to copy editing and page composition. It may differ from the final official version of record.

caused the phenol absorbance to increase in absorbance (55%) and shift to 457 nm ($\Delta\lambda_{max}$ = 40 nm). In contrast, the phenolate absorbance shifted to 570 nm ($\Delta\lambda_{max}$ = 35 nm) with ~ 78% loss in absorbance.

Excitation of the MN4-bound probe at 457 nm afforded relatively weak broad emission at 524 nm (green trace, Figure 3B). Extending the excitation wavelength toward the phenolate absorbance at 570 nm caused impressive growth in phenolate emission at 589 nm (orange traces, Figure 3B). However, compared to the HCs bearing electron-withdrawing halogen substituents, PhOBtz, Me_2PhOBtz and $(MeO)_2$PhOBtz afford relatively weak emission readout (Φ_{fl} ranging from 0.01-0.18) upon binding MN4 at pH 7.4 due to the dominance of the phenolic form. These results also demonstrate that placement of the phenolic HCs within the hydrophobic binding pocket of MN4 increases the ground-state pK_a of the dye to favor the protonated form, which is consistent with ΔpK_a values for phenols in water versus less-polar media (pK_a of phenol is ~ 10 in water versus 14 in MeOH).[32]

© The Author(s) or their Institution(s)

Can. J. Chem. Downloaded from cdnsciencepub.com by YORK UNIV on 07/12/24
For personal use only. This Just-IN manuscript is the accepted manuscript prior to copy editing and page composition. It may differ from the final official version of record.

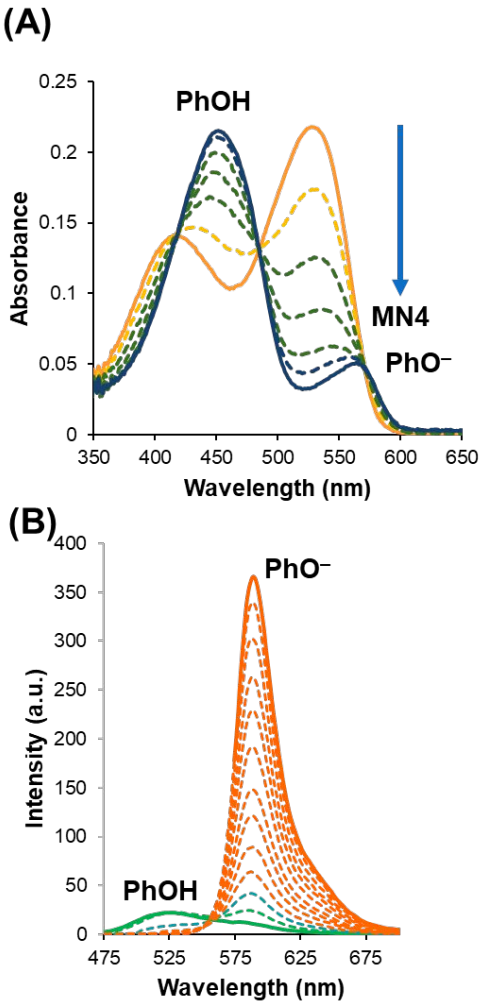


Figure 3. (A) UV-vis titration of Me_2PhOBtz (5 μM) with MN4 (added in 0.2 equiv. additions) and (B) Emission spectra of Me_2PhOBtz bound to MN4 recorded at excitation wavelengths from 400-570 nm. Spectra were acquired in PBS pH 7.4 at 20 ˚C.

To provide information on the location of the HC binding site in the MN4 aptamer, the ability of the quinine guest to directly displace the HCs from MN4 was investigated using UV-vis measurements. Quinine binds to the 3WJ of MN4 with a K_d of 0.21 μM. As noted previously for FPhOBtz displacement from MN4 through quinine additions,[19] the alkaloid target was able to readily displace PhOBtz, $(MeO)_2$PhOBtz and Cl_2PhOBtz from the 3WJ binding site of MN4 (Figure S4, SM), as these dyes all possess weaker affinity for MN4 compared to quinine. However, under similar conditions

© The Author(s) or their Institution(s)

Can. J. Chem. Downloaded from cdnsciencepub.com by YORK UNIV on 07/12/24
For personal use only. This Just-IN manuscript is the accepted manuscript prior to copy editing and page composition. It may differ from the final official version of record.

quinine was unable to displace Me_2PhOBtz from MN4, as the dimethyl analog possesses a K_d of 0.04 μM, which is ~ 5-fold greater than the quinine affinity. The specificity of the dyes and quinine target for the 3WJ of MN4 is ascribed to the hydrophobic effect, which is regarded as most important for host-guest binding in water.[33] This effect was originally explained in terms of a favourable entropy change arising from the liberation of ordered water molecules upon desolvation of the host and guest upon binding.[34] However, our ITC data indicates that binding of quinine and the dyes to MN4 is enthalpically driven with negative ΔH values and an unfavorable binding entropy (Table 2). The dominance of ΔH in the binding of hydrophobic guests has been ascribed to the release of "high energy" water molecules into a more favourable bulk solvation environment.[34] The hydrophobic 3WJ of MN4 affords a favorable binding pocket for numerous guest molecules, making it a highly promiscuous DNA aptamer.

Changes in the imino proton region of MN4 upon binding Me_2PhOBtz (Figure 4) confirmed dye binding to the 3WJ. Diagnostic features of dye binding to MN4 include the upfield shift of the G31 imino proton (labelled with the blue star for MN4; red circle for dye-bound MN4, Figure 4) and the upfield shift of the T18 imino proton, which are both located at or adjacent to the 3WJ. For MN4 binding by Me_2PhOBtz, distinct imino proton resonances for free MN4 and dye-bound MN4 were observed, indicating that the free and bound aptamer states are in slow exchange, which is consistent with strong dye binding. Overall, the quinine displacement studies and ^{1}H NMR titration data confirm 3WJ binding specificity by the HC dye family. Thus, although the different phenolic substituents strongly alter the physicochemical properties of the HC dyes (Table 1), they do not alter the binding specificity of the dyes for the 3WJ of MN4.

© The Author(s) or their Institution(s)

Can. J. Chem. Downloaded from cdnsciencepub.com by YORK UNIV on 07/12/24
For personal use only. This Just-IN manuscript is the accepted manuscript prior to copy editing and page composition. It may differ from the final official version of record.

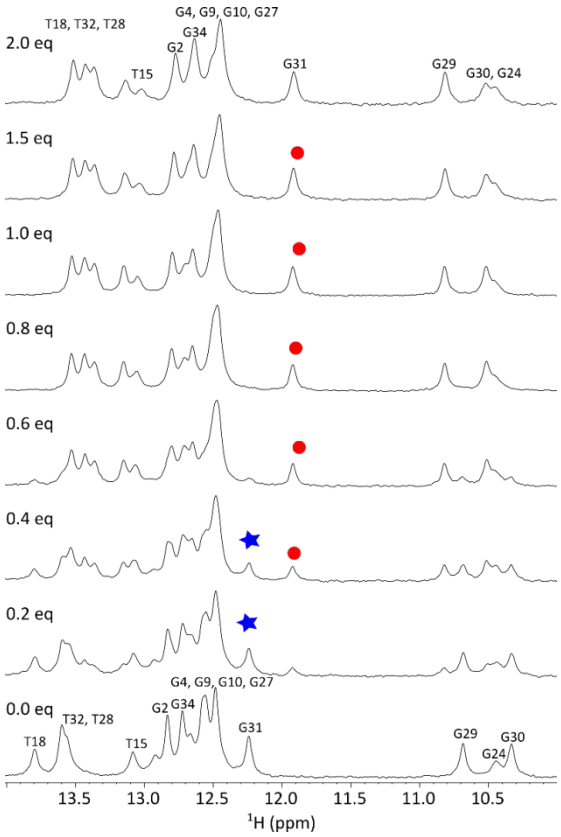


Figure 4. ^{1}H NMR titration of $Me_2PhOBtz$ into MN4 highlighting the imino proton resonances of the aptamer. Ratios on the spectrum denote the molar ratio of aptamer to $Me_2PhOBtz$. Spectra were acquired with an MN4 concentration of 1.4 mM in 140 mM NaCl, 10 mM Na_xH_yPO4, pH 6.8, 10% D_2O–90% H_2O at 5 ˚C. Upon addition of $Me_2PhOBtz$, the G31 resonance of free MN4 is highlighted by the blue star, while the $Me_2PhOBtz$-bound MN4 is highlighted by the red dot.

© The Author(s) or their Institution(s)

Can. J. Chem. Downloaded from cdnsciencepub.com by YORK UNIV on 07/12/24
For personal use only. This Just-IN manuscript is the accepted manuscript prior to copy editing and page composition. It may differ from the final official version of record.

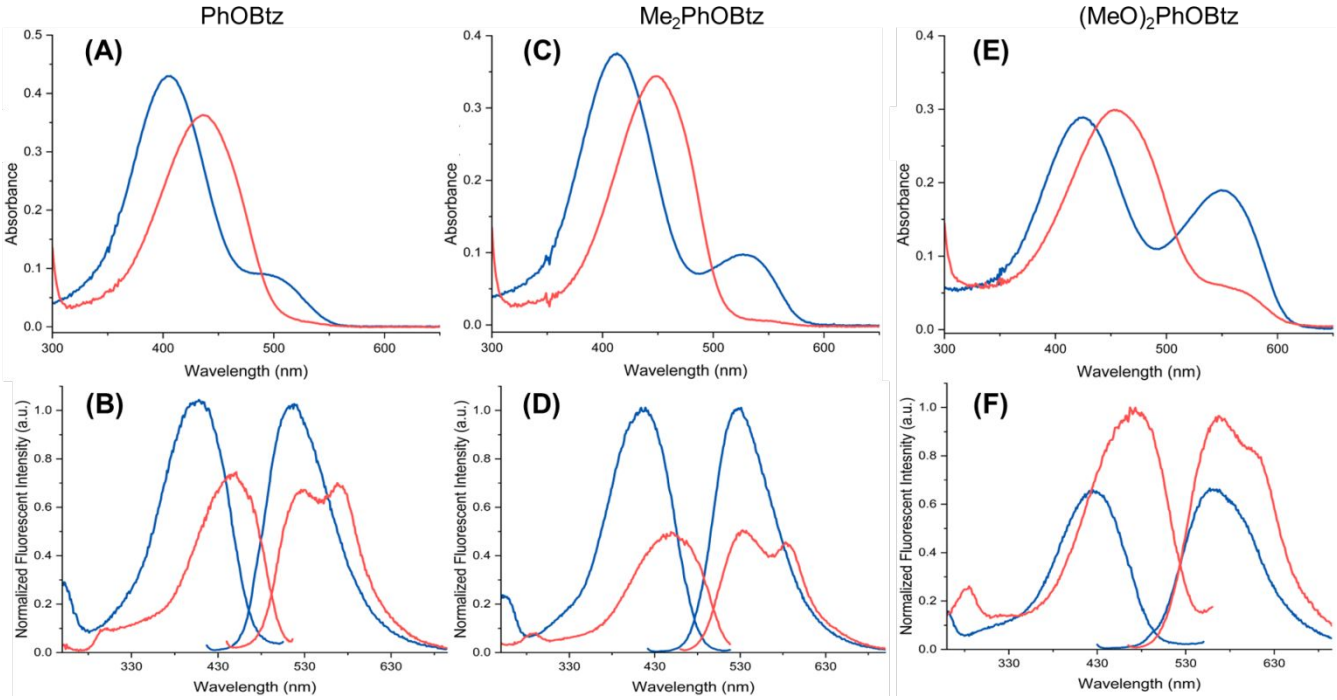


Figure 5. Absorbance (A, C and E) and fluorescence spectra (B, D and F) of HCs (5 μM) in the absence (blue traces) and presence (red traces) of MN4 (2 equiv) in MES buffer pH 6.5 at 20 ˚C.

Ratiometric Detection of Quinine at pH 6.5. To optimize ratiometric detection of quinine using PhOBtz, Me_2PhOBtz and $(MeO)_2$PhOBtz, the pH of the solution was lowered to 6.5 to facilitate single phenol absorbance upon dye binding to MN4. Under these conditions it was expected that phenol excitation of the MN4-bound dyes would yield both phenol and phenolate emission due to ESPT given the photoacidity of the phenolic HCs (Table 1). All three dyes display dual absorption bands due to phenol and phenolate at pH 6.5 (blue traces, Figure 5A, C, and E). Upon addition of 2 equiv MN4 (red traces) the phenolate absorbance of PhOBtz disappeared and the phenolic absorbance red-shifted with decreased intensity (Figure 5A). The absorbance of the Me_2PhOBtz dye responded in a similar fashion to MN4 binding, although a trace amount of phenolate absorbance remained (Figure 5C). The $(MeO)_2$PhOBtz dye exhibited the greatest amount of phenolate absorbance in both the free and MN4-bound state (Figure 5E).

© The Author(s) or their Institution(s)

Can. J. Chem. Downloaded from cdnsciencepub.com by YORK UNIV on 07/12/24
For personal use only. This Just-IN manuscript is the accepted manuscript prior to copy editing and page composition. It may differ from the final official version of record.

In the free state all three HCs displayed single phenol emission from phenol excitation with no evidence for ESPT (blue traces, Figures 5B, D and F). However, upon MN4 binding clear evidence for dual emission stemming from phenol excitation was observed (red traces), suggesting that placement of the dyes within the 3WJ of MN4 promotes ESPT. For PhOBtz (Figure 5B) the excitation wavelength shifted to the red with decreased intensity (30% quenched) compared to the free state. The emission displayed both phenol and phenolate bands of almost equal intensity, slightly favouring phenolate emission. The emission response of Me_2PhOBtz (Figure 5D) was similar, but the emission of the MN4-bound dye was more strongly quenched compared to the free state (~ 50%) and the dual emission slightly favoured phenol emission. In contrast, $(MeO)_2$PhOBtz (Figure 5F) displayed turn-on emission upon MN4 binding and dual emission was poorly resolved with phenolate emission appearing as a shoulder peak of weaker intensity compared to phenol emission.

The ability of quinine to directly displace PhOBtz from the 3WJ of MN4 at pH 6.5 was investigated using emission intensity measurements (Figure 6). For this experiment PhOBtz (5 μM) was mixed with 2 equiv aptamer and ligand binding was assessed through gain of PhOBtz emission intensity, due to competitive binding by the quinine guest to the 3WJ binding domain. Quinine-mediated displacement of PhOBtz caused preferential gain in phenol emission (2-fold enhancement) at the expense of phenolate emission and afforded a K_d of 14 μM (see Figure S5, SI) with a limit of detection (LOD) of 0.29 μM, which had similar sensitivity to the turn-off emission intensity response through FPhOBtz displacement by quinine (LOD ≈ 0.13 μM).[19] However, the turn-on response by PhOBtz bound to MN4 at pH 6.5 for quinine detection is much more advantageous for detection of biological analytes, as turn-off fluorescent detection platforms suffer from high background signal.[35]

A rationale for the fluorescent properties of the phenolic HCs bound to MN4 can be obtained from photophysical studies dealing with the emission of GFP and its analogs. The neutral phenolic

© The Author(s) or their Institution(s)

Can. J. Chem. Downloaded from cdnsciencepub.com by YORK UNIV on 07/12/24
For personal use only. This Just-IN manuscript is the accepted manuscript prior to copy editing and page composition. It may differ from the final official version of record.

chromophore in GFP absorbs at ~ 398 nm, while the anionic phenolate absorbs at ~ 478 nm.[36] The phenolic pK_a of the GFP chromophore is ~ 8 and excitation of GFP at either the phenol or phenolate peak affords green phenolate emission at ~ 508 nm. The ability of phenol excitation to generate phenolate emission is due to an ultrafast ESPT process on a picosecond time scale.[37] Within the GFP β-

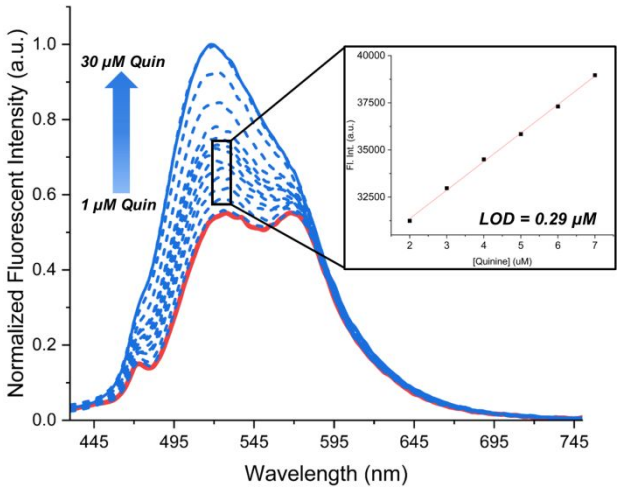


Figure 6. Fluorescence titration of quinine-mediated displacement of PhOBtz (5 μM) from MN4 (10 μM). Titration with quinine (6 equiv vs. [PhOBtz]) was carried out in MES pH 6.5 at 21 ˚C. The red trace is the initial emission of PhOBtz bound to MN4. Insert shows the linear range for the titration used to determine LOD.

barrel, a glutamate residue is the eventual proton acceptor from the excited GFP chromophore. For a highly fluorescent locked BF_2-mimic of the GFP chromophore (pK_a = 6.4, pK_a* ~ 0.6), Baranov and coworkers investigated its ESPT in MeOH/water mixtures and in water containing sodium acetate to mimic proton acceptance for the natural GFP chromophore within the protein.[38] No ESPT from the photoacid was observed in pure methanol, while in water bands for phenol and phenolate were noted (~1:1.9 ratio for PhOH:PhO^-). Addition of sodium acetate to the aqueous solution accelerated the observed ESPT and only phenolate emission was present in 3M sodium acetate solution, suggesting that a 3M acetate concentration may mimic the chromophore-COO^- interaction within the protein.[38]

© The Author(s) or their Institution(s)

Can. J. Chem. Downloaded from cdnsciencepub.com by YORK UNIV on 07/12/24
For personal use only. This Just-IN manuscript is the accepted manuscript prior to copy editing and page composition. It may differ from the final official version of record.

For the *O*-donor HCs in MES buffer at pH 6.5, no evidence for ESPT was observed. Under this scenario, the protolytic dissociation time must be longer than the fluorescence decay rate for R*OH. Upon binding the 3WJ of MN4, the dyes are shielded from the bulk aqueous media, placed in a more hydrophobic environment, and the phenolic portion of the dye may be in close contact with negatively charged phosphates and/or neutral nitrogen atoms of the nucleobases, possibly *N*3 of C_{20} located in the

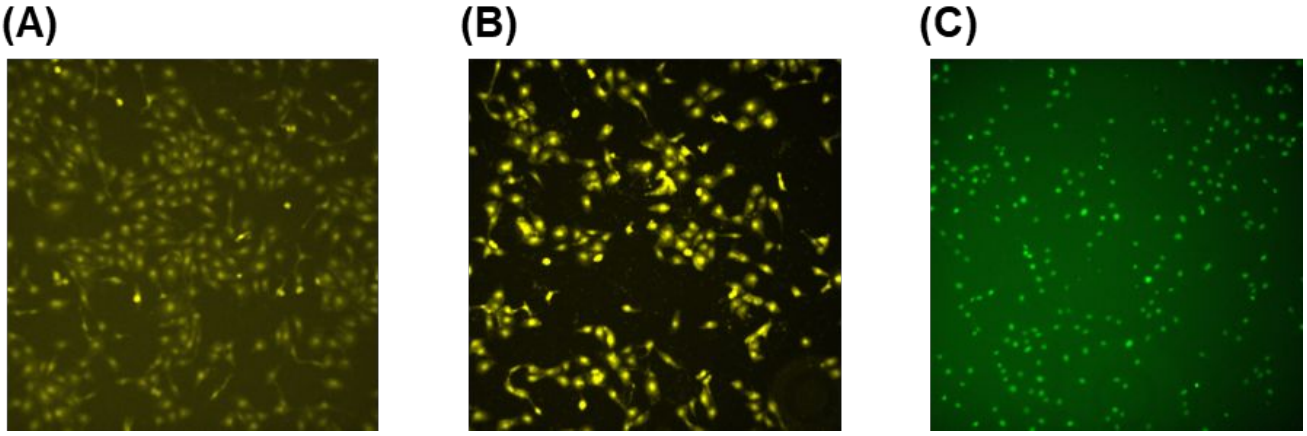


Figure 7. Composite BF-fluorescent imaging using (A) FPhOBtz, (B) Cl_2PhOBtz, and (C) $(MeO)_2$PhOBtz in live ovarian cancer cells (SKOV3). All dye solutions were at a 3μM concentration and were imaged following a 30 minutes incubation at 37 ˚C.

3WJ of MN4 (Figure 1). The pK_a of phosphate in DNA is ~ 1.0,[39] while the pK_a of the conjugate acid of dC is ~ 4.5,[40] and both are stronger proton acceptors than neutral water in the bulk solvent. Thus, phenolic HC binding to MN4 alters the photophysical properties of the dyes, which are now able to dissociate within the short lifetime of the phenolic excited state to generate two excited-state forms from a single phenolic ground-state, as required for ratiometric sensing (Figure 6).[9]

Cellular Imaging. The ability of the *O*-donor HCs to image DNA in a cellular environment (Figure 7) was assessed using the bright phenolate dyes (FPhOBtz and Cl_2PhOBtz) versus the phenolic dye $(MeO)_2$PhOBtz, which has been previously demonstrated to stain nuclear DNA with green fluorescence

© The Author(s) or their Institution(s)

Can. J. Chem. Downloaded from cdnsciencepub.com by YORK UNIV on 07/12/24
For personal use only. This Just-IN manuscript is the accepted manuscript prior to copy editing and page composition. It may differ from the final official version of record.

due to phenol excitation.[41] Overall, the phenolate dyes emit stronger signals when compared to the phenolic dye, as expected from their superior quantum yields upon DNA binding (Table 2). The Cl_2PhOBtz (Figure 7B) exhibits the strongest signal and best nucleus localization with minimal background signal. The FPhOBtz analog (Figure 7A) also displayed nucleus localization, but the image is poorly resolved compared to Figure 7B and contains greater background signal due to staining in the cytoplasm. The phenolic dye $(MeO)_2$PhOBtz (Figure 7C) exhibits weaker signal compared to Cl_2PhOBtz (Figure 7B), but displays better localization in the nucleus compared to FPhOBtz (Figure 7A). These experiments highlighted the ability of phenolic HCs to serve as nuclear stains in live cells and the ability to tune their performance through alteration of the *ortho*-substituents on the phenolic ring.

Conclusions

Our work demonstrates the tunability of phenolic HCs bearing the cationic N-methylbenzothiazolium (Btz) acceptor as turn-on fluorescent probes for DNA biosensing and cellular bioimaging applications. Promotion of phenolate formation by attaching halogens to the *ortho*-positions of the phenolic donor promotes strong turn-on fluorescence upon binding to the hydrophobic 3WJ of the quinine-binding aptamer MN4. For host-guest sensing applications displacement of the phenolate dye by the quinine target promotes a turn-off emission response, which is not ideal for detecting biological analytes due to the high background signal. However, the bright turn-on response of the phenolate HC upon DNA binding was advantageous for staining nuclear DNA in live ovarian cancer cells with high resolution. For this application the more lipophilic Cl_2PhOBtz outperformed the FPhOBtz derivative. The parent phenolic HC (PhOBtz) and those bearing electron-donating groups ($(MeO)_2$PhOBtz and Me_2PhOBtz) afforded dual absorbance and fluorescence at pH 7.4 due to the presence of the phenol and the

© The Author(s) or their Institution(s)

Can. J. Chem. Downloaded from cdnsciencepub.com by YORK UNIV on 07/12/24
For personal use only. This Just-IN manuscript is the accepted manuscript prior to copy editing and page composition. It may differ from the final official version of record.

phenolate. At pH to 6.5, PhOBtz generated a single phenolic absorbance peak when bound to the 3WJ of MN4. Unexpectedly, the fluorescence of PhOBtz bound to MN4 was quenched compared to the free dye and displayed both phenol and phenolate emission, while the free probe displayed only single phenolic emission from phenolic excitation. This observation suggested that DNA basic components within the 3WJ of MN4 served as the proton acceptor to facilitate ESPT from the excited phenol to generate phenolate emission. Thus, PhOBtz binding to MN4 with subsequent displacement by quinine afforded a turn-on ratiometric fluorescent response in a host-guest DNA detection platform, which is more advantageous for detecting biological analytes than a turn-off fluorescent readout. However, the relatively weak emission of the phenolic form of the HCs, as exemplified using $(MeO)_2$PhOBtz, was less effective than the phenolate for nuclear staining in ovarian cancer cells, highlighting the tuneability of phenolic HCs in DNA biosensing and bioimaging applications.

Acknowledgement: This contribution is in celebration of 150 years of chemistry at the University of Guelph (UofG). R.A.M. is grateful to the Department of Chemistry at UofG for continuous support since his hire in 2004.

Supplemental Material: Figures S1-S4 described in the text and NMR and HRMS spectra of synthetic dyes.

Competing Interests: The authors declare there are no competing interests.

Author Contributions: The manuscript was written through contributions of all authors, and all authors have given approval to the final version of the manuscript before the submission.

© The Author(s) or their Institution(s)

Can. J. Chem. Downloaded from cdnsciencepub.com by YORK UNIV on 07/12/24
For personal use only. This Just-IN manuscript is the accepted manuscript prior to copy editing and page composition. It may differ from the final official version of record.

Data Availability: Data generated or analyzed during this study are provided in full within the published article and its supplementary materials.

Funding: This work was supported by the Natural Sciences and Engineering Research Council (NSERC) of Canada (DG grants RGPIN-2018-06381 to P.E.J., RGPIN-2022-04563 to S.N.K. and RGPIN-2018-400136 to R.A.M.).

References

(1) Lee, S.-C.; Heo, J.; Woo, H. C.; Lee, J.-A.; Seo, Y. H.; Lee, C.-L.; Kim, S.; Kwon, O.-P. Fluorescent Molecular Rotors for Viscosity Sensors. *Chem. Eur. J.* **2018**, *24*, 13706–13718.

(2) Johnson, R. E.; Murray, M. T.; Bycraft, L. J.; Wetmore, S. D.; Manderville, R. A. A Modular Aldol Approach for Internal Fluorescent Molecular Rotor Chalcone Surrogates for DNA Biosensing Applications. *Chem. Sci.* **2023**, *14*, 4832–4844.

(3) Zeng, Z.; Liew, S. S.; Wei, X.; Pu, K. Hemicyanine-Based Near-Infrared Activatable Probes for Imaging and Diagnosis of Diseases. *Angew. Chem. Int. Ed.* **2021**, *60*, 2-24.

(4) Sun, W.; Guo, S.; Hu, C.; Fan, J.; Peng, X. Recent Development of Chemosensors Based on Cyanine Platforms. *Chem. Rev.* **2016**, *116*, 7768−7817.

(5) Chung, A. J.; Deore, P. S.; Al-Abdul-Wahid, S.; Aboelnga, M. M.; Wetmore, S. D.; Manderville, R. A. Acceptor Influence on Thiolate Sensing by Hemicyanine Dyes. *J. Org. Chem.* **2019**, *84*, 2261-2268.

© The Author(s) or their Institution(s)

Can. J. Chem. Downloaded from cdnsciencepub.com by YORK UNIV on 07/12/24
For personal use only. This Just-IN manuscript is the accepted manuscript prior to copy editing and page composition. It may differ from the final official version of record.

(6) Johnson, R. E.; Murray, M. T.; Bycraft, L. J.; Myler, P.; Wetmore, S. D.; Manderville, R. A. Harnessing a 4-Formyl-Aniline Handle to Tune the Stability of a DNA Aptamer-Protein Complex via Fluorescent Surrogates. *Bioconjugate Chem.* **2023**, *34*, 2066-2076.

(7) Deore, P. S.; Gray, M. D.; Chung, A. J.; Manderville, R. A. Ligand-Induced G-Quadruplex Polymorphism: A DNA Nanodevice for Label-Free Aptasensor Platforms. *J. Am. Chem. Soc.* **2019**, *141*, 14288-14297.

(8) Haidekker, M. A; Theodorakis, E. A. Ratiometric Mechanosensitive Fluorescent Dyes: Design and Applications. *J. Mater. Chem. C* **2016**, *4*, 2707-2718.

(9) Michel, B. Y.; Dziuba, D.; Benhida, R.; Demchenko, A. P.; Burger, A. Probing of Nucleic Acid Structures, Dynamics, and Interactions with Environment-Sensitive Fluorescent Labels. *Front. Chem.* **2020**, *8*, 112.

(10) Wu, L.; Huang, C.; Emery, B. P.; Sedgwick, A. C.; Bull, S. D.; He, X-P.; Tian, H.; Yoon, J.; Sessler, J. L.; James, T. D. Förster Resonance Energy Transfer (FRET)-Based Small-Molecule Sensors and Imaging Agents. *Chem. Soc. Rev.* **2020**, *49*, 5110-5139.

(11) Blanchard, D. J. M.; Cservenyi, T. Z.; Manderville, R. A. Dual Fluorescent Deoxyguanosine Mimics for FRET Detection of G-Quadruplex Folding. *Chem. Commun.* **2015**, *51*, 16829-16831.

(12) Wang, C.; Jiang, W.; Tan, D.; Huang, L.; Li, J.; Qiao, Q.; Yadav, P.; Liu, X.; Xu, Z. Monitoring Amyloid Aggregation via a Twisted Intramolecular Charge Transfer (TICT)-Based Fluorescent Sensor Array. *Chem. Sci.* **2023**, *14*, 4786–4795.

© The Author(s) or their Institution(s)

Can. J. Chem. Downloaded from cdnsciencepub.com by YORK UNIV on 07/12/24
For personal use only. This Just-IN manuscript is the accepted manuscript prior to copy editing and page composition. It may differ from the final official version of record.

(13) Okamoto, A.; Tainaka, K.; Nishiza, K.-I.; Saito, I. Monitoring DNA Structures by Dual Fluorescence of Pyrene Derivatives. *J. Am. Chem. Soc.* **2005**, *127*, 13128–13129.

(14) Sedgwick, A. C.; Wu, L.; Han, H.-H.; Bull, S. D.; He, X.-P.; James, T. D.; Sessler, J. L.; Tang, B. Z.; Tian, H.; Yoon, J. Excited-State Intramolecular Proton-Transfer (ESIPT) Based Fluorescence Sensors and Imaging Agents. *Chem. Soc. Rev.* **2018**, *47*, 8842–8880.

(15) Dziuba, D.; Postupalenko, V. Y.; Spadafora, M.; Klymchenko, A. S.; Guérineau, V.; Mély, Y.; Benhida, R.; Burger, A. A Universal Nucleoside with Strong Two-Band Switchable Fluorescence and Sensitivity to the Environment for Investigating DNA Interactions. *J. Am. Chem. Soc.* **2012**, *134*, 10209-10213.

(16) Regan, K. T.; Pounder, A.; Lin, C.; Chen, L. D.; Manderville, R. A. Isomer-Specific Solvatochromic and Molecular Rotor Properties of ESIPT-Active Push-Pull Fluorescent Chalcone Dyes. *J. Phys. Chem. A* **2023**, *127*, 8365-8373.

(17) Li, Y.; Dahal, D.; Abeywickrama, C. S.; Pang, Y. Progress in Tuning Emission of the Excited-State Intramolecular Proton Transfer (ESIPT)-Based Fluorescent Probes. *ACS Omega* **2021**, *6*, 6547–6553.

(18) Van Riesen, A. J.; Johnson, R. E.; Al-Abdul-Wahid, S.; Liota, C.; Christyanton, A.; Manderville, R. A. Temperature Sensing of Thiolate Addition by Phenolate Merocyanine Dyes: Importance of the Quinone Methide Resonance Structure. *J. Org. Chem.* **2021**, *86*, 1583-1590.

(19) Van Riesen, A. J.; Le, J.; Slavkovic, S.; Churcher, Z. R.; Shoara, A. A.; Johnson, P. E.; Manderville, R. A. Visible Fluorescent Light-up Probe for DNA Three-Way Junctions Provides Host–Guest Biosensing Applications. *ACS Appl. Bio Mater.* **2021**, *4*, 6732-6741.

© The Author(s) or their Institution(s)

Can. J. Chem. Downloaded from cdnsciencepub.com by YORK UNIV on 07/12/24
For personal use only. This Just-IN manuscript is the accepted manuscript prior to copy editing and page composition. It may differ from the final official version of record.

(20) Van Riesen, A. J.; Kalnitsky, B.; Shoara, A. A.; Slavkovic, S.; Churcher, Z. R.; Johnson, P. E.; Manderville, R. A. Tuning the DNA Binding properties of Phenolic Hemicyanine Dyes for Host-Guest Fluorescent Aptasensor Applications. *Dyes Pigm.* **2023**, *209*, 110936.

(21) Stojanovic, M. N.; de Prada, P.; Landry, D. W. Aptamer-Based Folding Fluorescent Sensor for Cocaine. *J. Am. Chem. Soc.* **2001**, *123*, 4928-4931.

(22) Neves, M. A. D.; Reinstein, O.; Johnson, P. E. Defining a Stem Length-Dependent Binding Mechanism for the Cocaine-Binding Aptamer. A Combined NMR and Calorimetry Study. *Biochemistry* **2010**, *49*, 8478-8487.

(23) Reinstein, O.; Yoo, M.; Han, C.; Palmo, T.; Beckham, S. A.; Wilce, M. C. J.; Johnson, P. E. Quinine Binding by the Cocaine-Binding Aptamer. Thermodynamic and Hydrodynamic Analysis of High-Affinity Binding of an Off-Target Ligand. *Biochemistry* **2013**, *52*, 8652-8662.

(24) Churcher, Z. R.; Neves, M. A. D.; Hunter, H. N.; Johnson, P. E. Comparison of the Free and Ligand-Bound Imino Hydrogen Exchange Rates for the Cocaine-Binding Aptamer. *J. Biomol. NMR* **2017**, *68*, 33-39.

(25) Sun, K. M.; McLaughlin, C. K.; Lantero, D. R.; Manderville, R. A. Biomarkers for Phenol Carcinogen Exposure Act as pH-Sensing Fluorescent Probes. *J. Am. Chem. Soc.* **2007**, *129*, 1894-1895.

(26) Biggs, A. I.; Robinson, R. A. The Ionisation Constants of Some Substituted Anilines and Phenols: A Test of the Hammett Relation. *J. Chem. Soc.* **1961**, 388-392.

(27) Hansch, C.; Leo, A.; Taft, R. W. A Survey of Hammett Substituent Constants and Resonance and Field Parameters. *Chem. Rev.* **1991**, *91*, 165-195.

© The Author(s) or their Institution(s)

Can. J. Chem. Downloaded from cdnsciencepub.com by YORK UNIV on 07/12/24
For personal use only. This Just-IN manuscript is the accepted manuscript prior to copy editing and page composition. It may differ from the final official version of record.

(28) Förster, T. Die pH-Abhängigkeit der Fluoreszenz von Naphthalinderivaten. *Z. Electrochem.* **1950**, *54*, 531-535.

(29) Prémont-Schwarz, M.; Barak, T.; Pines, D.; Nibbering, E. T. J.; Pines, E. Ultrafast Excited-State Proton-Transfer Reaction of 1-Naphthol-3,6-Disulonate and Several 5-Substituted 1-Naphthol Derivatives. *J. Phys. Chem. B* **2013**, *117*, 4594-4603.

(30) Reichardt, C. Solvatochromic Dyes as Solvent Polarity Indicators. *Chem. Rev.* **1994**, *94*, 2319-2358.

(31) Singer, V. L.; Jones, L. J.; Yue, S. T.; Haugland, R. P. Characterization of PicoGreen Reagent and Development of a Fluorescence-Based Solution Assay for Double-Stranded DNA Quantitation. *Anal. Biochem.* **1997**, *249*, 228-238.

(32) Rossini, E.; Bochevarov, A. D.; Knapp, E. W. Empirical Conversion of pK_a Values between Different Solvents and Interpretation of the Parameters: Application to Water, Acetonitrile, Dimethyl Sulfoxide, and Methanol. *ACS Omega* **2018**, *3*, 1653-1662.

(33) Pratt, L. R.; Pohorille, A. Hydrophobic Effects and Modeling of Biophysical Aqueous Solution Interfaces. *Chem. Rev.* **2002**, *102*, 2671-2692.

(34) Metherell, A. J.; Cullen, W.; Williams, N. H.; Ward, M. D. Binding of Hydrophobic Guests in a Coordination Cage Cavity is Driven by Liberation of "High-Energy" Water. *Chem. Eur. J.* **2018**, *24*, 1554-1560.

(35) Zhou, J.; Ma, H. Design Principles of Spectroscopic Probes for Biological Applications. *Chem. Sci.* **2016**, *7*, 6309−6315.

© The Author(s) or their Institution(s)

Can. J. Chem. Downloaded from cdnsciencepub.com by YORK UNIV on 07/12/24
For personal use only. This Just-IN manuscript is the accepted manuscript prior to copy editing and page composition. It may differ from the final official version of record.

(36) Ward, W. W.; Bokman, S. H. Reversible Denaturation of *Aequorea* Green-Fluorescent Protein: Physical Separation and Characterization of the Renatured Protein. *Biochemistry* **1982**, *21*, 4535-4540.

(37) Chattoraj, M.; King, B. A.; Bublitz, G. U.; Boxer, S. G. Ultra-fast Excited State Dynamics in Green Fluorescent Protein: Multiple States and Proton Transfer. *Proc. Natl. Acad. Sci. U.S.A.* **1996**, *93*, 8362-8367.

(38) Baranov, M. S.; Lukyanov, K. A.; Borissova, A. O.; Shamir, J.; Kosenkov, D.; Slipchenko, L. V.; Tolbert, L. M.; Yampolsky, I. V.; Solntsev, K. M. Conformationally Locked Chromophores as Models of Excited-State Proton Transfer in Fluorescent Proteins. *J. Am. Chem. Soc.* **2012**, *134*, 6025-6032.

(39) Thaplyal, P.; Bevilacqua, P. C. Experimental Approaches for Measuring pK_a's in RNA and DNA. *Methods Enzymology*. **2014**, *549*, 189-219.

(40) Christensen, J. J.; Rytting, J. H.; Izatt, R. M. Thermodynamics of Proton Dissociation in Dilute Aqueous Solution. VIII. pK, ΔH°, and ΔS° Values for Proton Ionization from Several Pyrimidines and Their Nucleosides at 25°. *J. Phys. Chem.* **1967**, *71*, 2700-2705.

(41) Yang, R.; He, X.; Niu, G.; Meng, F.; Lu, Q.; Liu, Z.; Yu, X. A Single Fluorescent pH Probe for Simultaneous Two-Color Visualization of Nuclei and Mitochondria and Monitoring Cell Apoptosis. *ACS Sens.* **2021**, *6*, 1552-1559.

© The Author(s) or their Institution(s)